frontiers | Frontiers in Energy Research

TYPE Original Research
PUBLISHED 13 January 2023
DOI 10.3389/fenrg.2022.1042391

OPEN ACCESS

EDITED BY
Mingjun Wang,
Xi'an Jiaotong University, China

REVIEWED BY
Haochun Zhang,
Harbin Institute of Technology, China
Zhuqiang Yang,
Dalian University of Technology, China

*CORRESPONDENCE
Shanfang Huang,
sfhuang@mail.tsinghua.edu.cn

SPECIALTY SECTION
This article was submitted to Nuclear Energy, a section of the journal Frontiers in Energy Research

RECEIVED 12 September 2022
ACCEPTED 14 November 2022
PUBLISHED 13 January 2023

CITATION
Liu M, Liu S, Xi D, Huang S and Huang Y (2023), Analysis of heat transfer mechanism in supercritical fluids from the aspect of pool heating.
Front. Energy Res. 10:1042391.
doi: 10.3389/fenrg.2022.1042391

Analysis of heat transfer mechanism in supercritical fluids from the aspect of pool heating

Minyun Liu[1,2], Shenghui Liu[3], Dapeng Xi[1], Shanfang Huang[2]* and Yanping Huang[1]

[1]CNNC Key Laboratory on Nuclear Reactor Thermal Hydraulics Technology, Nuclear Power Institute of China, Chengdu, China, [2]Department of Engineering Physics, Tsinghua University, Beijing, China, [3]Key Laboratory of Energy Thermal Conversion and Control of Ministry of Education, School of Energy and Environment, Southeast University, Nanjing, China

For the special phenomena of heat transfer deterioration or enhancement in supercritical fluid heat transfer, existing research still presents inconsistent opinions. In this study, we perform an analysis of the property changes, and present new understandings for pseudo-boiling theory. More importantly, essential differences between subcritical boiling and supercritical pseudo-boiling are highlighted; the critical factors being thermodynamic instability and stability. For isothermal heating cases, pseudo film boiling can be regarded as an extension of near-critical boiling. Moreover, pseudo nucleate boiling only appears in non-isothermal heating cases and is strongly dependent on the heater geometry, materials, etc. A coupled level-set and volume-of-fluid method is used to simulate the near-critical film boiling of carbon dioxide at pressures of 7.0 and 7.37 MPa. In comparison, supercritical cases at a pressure of 7.5 MPa are the natural convections of single-phase fluid with variable physical properties. The numerical results indicate the similar motions of low-density fluids in subcritical and supercritical cases. All results are consistent with prior experiments, providing a better understanding of the special features of supercritical fluid heat transfer.

KEYWORDS

supercritical fluids, pseudo-boiling, boiling, natural convection, heat transfer

1 Introduction

Fourth-generation nuclear energy systems are safer and more economical, and their use has gradually spread worldwide. Among different reactor designs, system simplification and the realization of a higher core outlet temperature is easier in gas-cooled reactors. Recently, supercritical carbon dioxide cooled reactors have aroused widespread attention because of advantages in efficiency, small size, and weight (Ahn et al., 2015). These advantages are due to the peculiar physicochemical properties of supercritical fluids (SCF), especially in the pseudo-critical region (Brun et al., 2017). However, special heat transfer mechanisms have also been found, which pose numerous risks to the system (Duffey and Pioro, 2005) and should be carefully studied. Similar problems exist in supercritical water reactors.

In the vicinity of the critical point, SCFs are very compressible and dense. For such fluids in heated enclosures, the rapid establishment of thermal equilibration, observed in microgravity experiments, cannot be explained by convection and conduction (Shen and Zhang, 2013). Onuki et al. (1990) (Boukari et al., 1990; Zappoli et al., 1990) studied dominant thermo-acoustic heating (piston effect) and successfully explained microgravity experiments through numerical models. However, for most industrial applications of SCF heat transfer, systems are maintained at a constant pressure using a pressurizer. In this condition, expansion of the thermal boundary layer cannot cause adiabatic compression of bulk materials, unlike a moving piston. Meanwhile, unlike the study of the piston effect at small temperature differences (dozens of milli Kelvins), fluid states are usually much removed from the critical point. These factors together make the piston effect negligible.

Therefore, buoyancy driven convection, including natural convection and mixed convection, is still the key driver of SCF heat transfer. Large-scale variations of SCF properties within the pseudo-critical region make the transfer mechanism complex, indicated by various experimental studies (Swenson et al., 1965; Li et al., 2010; Jiang et al., 2013). For heat transfer of SCFs flowing inside channels, Pioro and Duffey (2005) (Duffey and Pioro, 2005) reviewed more than 450 experimental papers on supercritical water and supercritical carbon dioxide spanning from the 1950s to the 2000s. The results verify that three different heat transfer modes dominate (Mokry et al., 2010): normal heat transfer, improved heat transfer, and deteriorated heat transfer. These modes are mainly influenced by the pressure, pipe diameter, mass flow rate, heat flux, bulk temperature, and flow direction. Similar phenomena are also observed in other SCFs, for example, methane (Gu et al., 2013) and kerosene (Fu et al., 2017). For natural convection of SCFs, Knapp and Sabersky (Knapp and Sabersky, 1966) designed an experiment employing horizontal wires heated in supercritical carbon dioxide. In the experiment, three general types of flow modes were observed: laminar flow, oscillation flow, and bubble-like flow, which are similar to subcritical pool boiling. Since then, many studies (Goldstein and Aung, 1968; Nishkawa and Ito, 1969; Abadzic and Goldstein, 1970; Neumann and Hahne, 1980) have attempted to repeat Knapp's work, and it was finally determined that the last two modes only appear in experiments that heat thin, low thermal diffusivity wires (Hahne and Neumann, 1981).

From a theoretical perspective, the mechanisms for improved heat transfer and deteriorated heat transfer are still controversial. According to observations of bubble-like structures and flow noise such as subcritical boiling, some studies (Ackerman, 1970; Banuti and Hannemann, 2014; Nasuti and Pizzarelli, 2020; Xu et al., 2020) proposed a pseudo-boiling theory and likened the improved heat transfer to nuclear boiling, and the deteriorated heat transfer to film boiling. Another theory focused on the buoyancy and flow acceleration effects caused by changes in the properties (McEligot et al., 1970; Petukhov et al., 1972; Hiroaki et al., 1973; Liu et al., 2017; Xu et al., 2017). This theory considers the force on near-wall fluids and explains experiment results very well. Nevertheless, the two theories have limitations. Existing research still presents inconsistent results, especially regarding the onset of heat transfer deterioration. For the pseudo-boiling theory, differences between the subcritical gas-liquid transition and pseudo-critical phenomena should be carefully considered. For the buoyancy and flow acceleration theory, effects of peculiar properties on the boundary layer are important and difficult to elucidate, requiring further studies.

Many researchers have carried out both experimental and theoretical studies on SCF heat transfer, particularly on flow and heat transfer in tubes. However, the existing research still yields inconsistent results due to complex turbulence flows. In contrast, it is much simpler to conduct visual experiments on, and to analyze the mechanism in pool heating cases; rarely reported in existing SCF studies. Moreover, basic analyses of the property distortions, especially comparisons of the subcritical gas-liquid transition, can also provide important information. Therefore, in the present study, the similarities of, and differences between the subcritical gas-liquid transition and pseudo-critical phenomena are studied using theoretical analyses and numerical simulations. A coupled level-set and volume-of-fluid method is used to analyze bubble growth in the film boiling of carbon dioxide near its critical point. For cases above the critical point, the natural convection of single-phase fluid with variable properties is considered. Through comparisons of these cases, the pseudo-boiling heat transfer mechanism in supercritical fluids has been improved.

2 Analysis of heat transfer characteristics of supercritical fluid in pool heating cases

The original pseudo-boiling theory was advanced by experimental observations, and can partly be proved by comparing gas-liquid transitions and pseudo-critical transitions, especially similarities in property changes. However, more importantly, the discrepancies in thermodynamic stabilities between these transitions lead to essential differences; thus, the original pseudo-boiling theory must be modified.

2.1 Similarities between the subcritical gas-liquid transition and the pseudo-critical transition

Taking water as an example, Figure 1 displays several properties at different pressures, including the density ρ, isobaric heat capacity c_P, thermal conductivity λ, viscosity μ, isothermal compressibility κ_T and thermal expansion rate α_P.

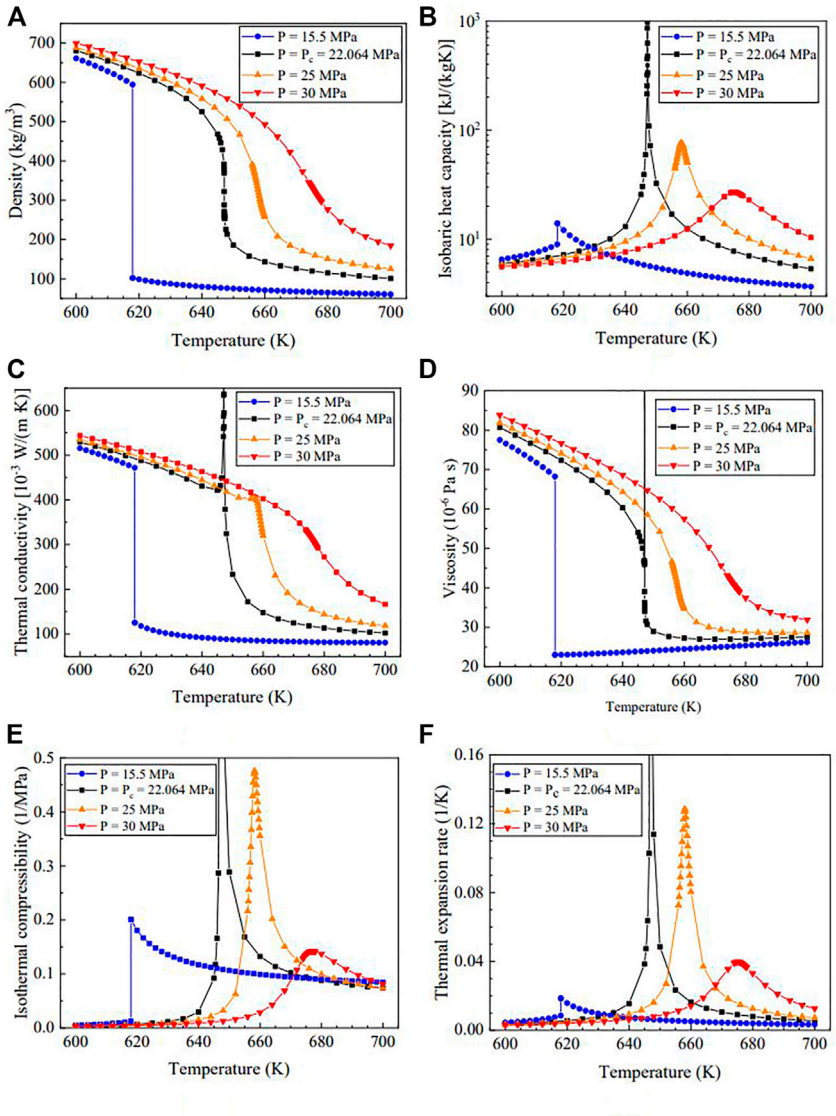

FIGURE 1
Different properties of water at different pressures.

The dotted line corresponds to the subcritical condition and the other three correspond to supercritical conditions. Many similarities between the subcritical gas-liquid transition and the pseudo-critical transition can be found from comparisons of the property changes.

Similar to the stepwise change during the subcritical gas-liquid transition, the fluid density changes dramatically in the pseudo-critical region. At a constant pressure of $P = 25$ MPa, the density of supercritical water changes from 400 kg/m^3 to 200 kg/m^3 over a 10 K temperature range. Meanwhile, the critical point is special where the first derivative $(\partial\rho/\partial T)_P$, and second derivative $(\partial^2\rho/\partial T^2)_P$, of the fluid density with respect to temperature are infinite.

For the isobaric heat capacity c_P, similarities also exist, but are more complex. The subcritical transition from the gas phase to liquid phase is accompanied by a jump in c_P. In the pseudo-critical transition, this phenomenon can also be observed, but is accompanied by a peak in c_P. Within the pseudo-critical region, c_P increases rapidly and then decreases as the temperature increases at a constant pressure. Specially, the unusual change of c_P at the critical pressure follows the power law $\Delta c_P \propto (T - T_C)^{-1.24}$, which is well explained by the scaling law (Kadanoff et al., 1967) and renormalization group (RG) theory (Wilson, 1971; Cardy, 1996). At the critical point, c_P is infinite. Away from the critical point, the c_P peak still exists, which corresponds to an additional energy demand for the

transition from high-density fluid to low-density fluid. The additional energy demand is quite similar to the latent heat of vaporization h_{lg}, in the subcritical gas-liquid transition, and can be quantitatively described by an integral of c_P with respect to T.

The isothermal compressibility, κ_T, and thermal expansion rate, α_P, are measures of the fluid density change as a response to a pressure or temperature change. The values of κ_T and α_P for a low-density fluid including the gas phase in subcritical states and gas-like fluid in supercritical states, are always higher than those for high-density fluids. Meanwhile, the peaks in κ_T and α_P in the pseudo-critical region refer to the peculiar change in fluid density.

The changes in the thermal conductivity, λ, and viscosity, μ, in supercritical states are similar to those in subcritical states. Compared with low-density fluids, a high-density fluid presents higher values of λ and μ. However, critical enhancement areas exist in the pseudo-critical region, corresponding to the peaks in Figures 1C,D. As the pressure increases away from the critical point, the dramatic changes in these properties are mild. Compared with those of c_P, the effects of the critical enhancement areas on λ and μ are much weaker and diminish quicker, and are usually negligible.

In the supercritical region, the maximum of the isobaric specific heat, c_p, at a constant pressure is called the pseudo-critical point, and is determined by the pseudo-critical pressure, P_{pc}, and the pseudo-critical temperature, T_{pc}. The pseudo-critical line connects these points and is also called the Widom line. In this context, the pseudo-critical line seems to be an extension of the gas-liquid coexistence line.

These phenomena are also present in other fluids, indicating the correlation between the subcritical gas-liquid transition and the pseudo-critical transition. Meanwhile, inelastic X-ray scattering experiments (Gorelli et al., 2006; Simeoni et al., 2010; Fomin et al., 2015) confirm the transitions between liquid-like and gas-like structures in SCFs, which are well reproduced by molecular dynamics simulations. Many studies (Ha et al., 2018; Yoon et al., 2019; Maxim et al., 2020) have examined structure-property correlations and have proposed the theory "supercritical gas-liquid coexistence" on a micro level. For different fluids in different states, intermolecular attraction and repulsion leads to different macro behaviors.

2.2 Differences between the subcritical gas-liquid transition and the pseudo-critical transition

Although many similarities between the two phenomena are presented above, the subcritical gas-liquid transition is still fundamentally different from the pseudo-critical transition (Liu et al., 2022). In the subcritical gas-liquid transition, phase separation occurs between gas and liquid phases and surface tension plays an important role in boiling. However, in the whole

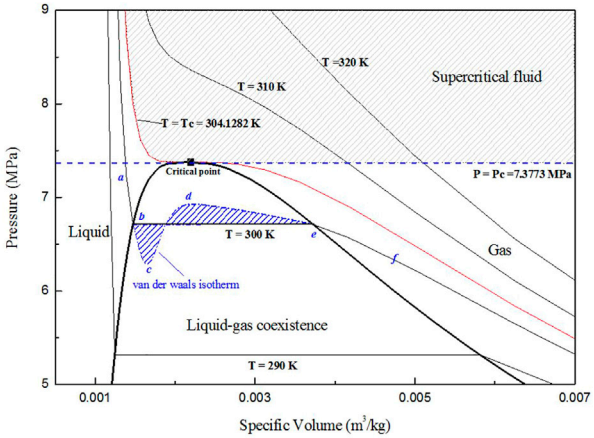

FIGURE 2
P-V diagram for carbon dioxide.

supercritical region, the two phases are indistinguishable, and phase separation does not occur. These differences can be explained by the thermodynamic stability theory and different heat transfer mechanisms.

According to the well-known van der Waals model, the isotherm is represented by "*abcdef*" in Figure 2. For *cd*, $(\partial P/\partial V)_T > 0$, which means that the pressure increases when the fluid volume increases. The states are unstable, leading to the separation and coexistence of gas and liquid phases. *bc* and *de* correspond to superheated liquid and subcooled gas, respectively, which are semi-stable and easily transition to the gas-liquid coexistence state. Therefore, for $T - T_C < 0$, the middle of the isotherm is a straight line, *be*. For $T - T_C > 0$, the isotherm is a monotonically decreasing function and $(\partial P/\partial V)_T < 0$. The states are always stable and the predictions of the van der Waals model are consistent with the experimental data.

In the subcritical pool boiling case, with heating from the bottom, the temperature of the heated wall is higher than the saturated temperature. At this condition, fluid near the wall is superheated. However, most of the superheated liquid cannot transform into gas as the formation of bubbles is conditional and random. The appearance of the gas phase in superheated liquid originates from density fluctuations caused by random movement of molecules. As illustrated in Figure 3A, density fluctuations cause a pressure increase, ΔP, in a region. If ΔP is large enough to overcome the surface tension, this region expands. As $(\partial P/\partial V)_T > 0$, expansion leads to a further increased pressure and the expansion continues until a stable, low-density state (a bubble) is formed. Generally, the initial unstable region (called a nucleation site) appears on the surface of the heated wall, where the effect of surface tension is relatively small.

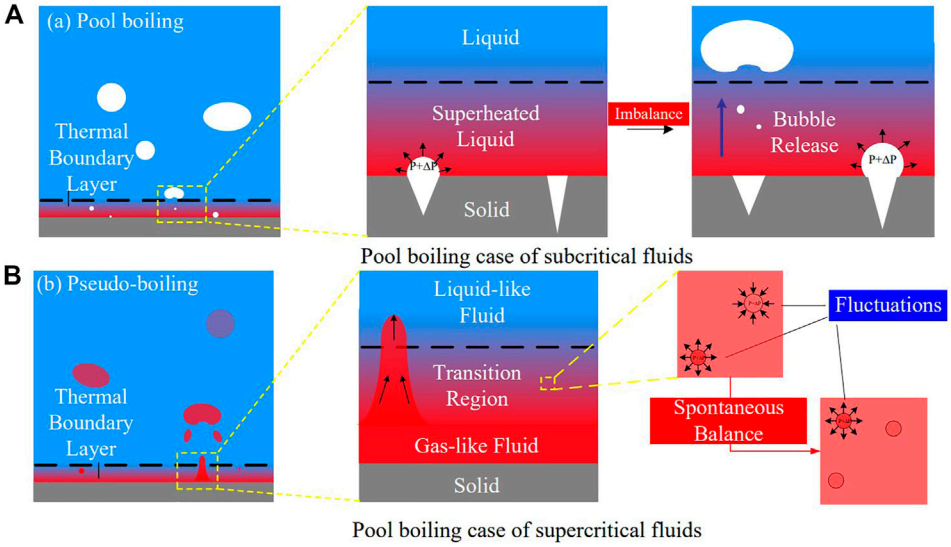

FIGURE 3
Different heat transfer mechanisms of the **(A)** subcritical gas-liquid transition and **(B)** pseudo-critical transition.

The pseudo-boiling case is referred to as the subcritical boiling case, where the bulk temperature is less than the pseudo-critical temperature, T_{pc}, and the wall temperature is higher. As illustrated in Figure 3B, fluid near the wall is low-density and the bulk is high-density. In the transition region between gas-like fluid and liquid-like fluid, the fluid density rapidly changes, corresponding to the pseudo-critical transition. Under the effect of buoyancy, the low-density fluid flows upward. The flow mode is similar to those of bubbles during boiling. However, the formation mechanisms of low-density fluids in pseudo-boiling and bubbles in boiling are different. As $(\partial P/\partial V)_T < 0$, fluctuations in SCFs dissipate spontaneously and do not destabilize the system. Gas-like and liquid-like structures are homogenously dispersed in the SCFs, originating from density fluctuations caused by the random movement of molecules. Thus, SCFs are always continuous and homogenous on a macro scale.

Subcritical gas-liquid transition depends on two key parameters: temperature and nucleation sites. Bubble formation is a stochastic process, dominated by density fluctuations and thermodynamic instability. Further, different modes of bubble formation and movement lead to different boiling modes, including nucleate boiling, transition boiling, and film boiling. The pseudo-critical transition depends on the temperature, and gas-like fluid formation is a deterministic process, although the movements of gas-like fluids are still stochastic. Different modes of gas-like fluid formation and movement also cause different pseudo-boiling modes. According to the prior similarity analyses, the pseudo-boiling modes are similar to the boiling modes. Natural convection induced by buoyancy, with a large density difference, is the common feature.

2.3 Mathematical description of hydraulic instability

For a typical subcritical horizontal film boiling case, a layer of vapor fully covers the heated wall and a layer of liquid is present above the vapor layer. The temperature of the heated wall is constant and higher than the saturation temperature. Due to density differences under gravity, the liquid-vapor interface is unstable, which is called Rayleigh-Taylor instability. Meanwhile, evaporation of the liquid and the generation of fresh vapor cause changes at the gas-liquid interface.

According to Taylor's theory (Taylor, 1950), the interface disturbance can be expressed through first-order perturbation analysis using the following equation:

$$\eta = \sum_k \eta_k e^{-in_k t} \cos kx = \sum_k \eta_k e^{b_k t} \cos kx \tag{1}$$

The growth coefficient, b_k, is related to the wave frequency, n_k; and the wavenumber, k, is related to the wavelength, l_k, by:

$$b_k = -in_k, \quad k = \frac{2\pi}{l_k} \tag{2}$$

Therefore, the interface disturbance is divided into several sub-disturbances with a particular wavelength l_k. When b_k is imaginary, the sub-disturbance is periodic in time and therefore

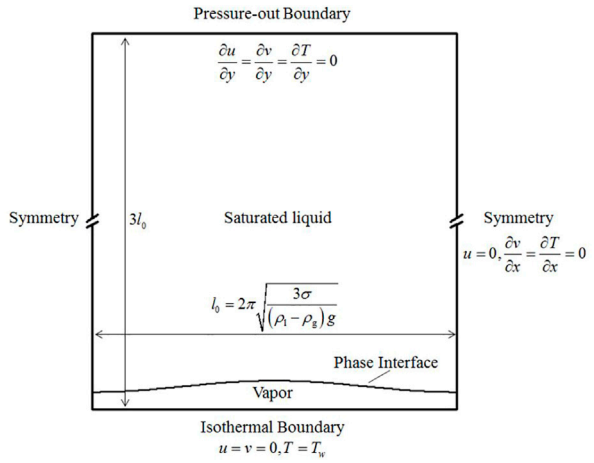

FIGURE 4
Computational domain and boundary conditions in subcritical cases.

stable. However, if b_m is real, the sub-disturbance grows exponentially with time and is therefore unstable.

For the horizontal film boiling with no forced convection, the irrotational flow kinematic equation, which yields the relations between wave number, gravity, surface tension, and the fluid properties, can be simplified to the following equation (Berenson, 1961):

$$k\rho_g\left(V_g-\frac{n_k}{k}\right)^2+k\rho_l\left(\frac{n_k}{k}\right)^2=g\sigma k^2-g\left(\rho_l-\rho_g\right) \tag{3}$$

If the vapor velocity, V_v, is negligible, then the equation for the grow coefficient b is:

$$b_k^2=-n_k^2,\ b_k=\left[\frac{g\left(\rho_l-\rho_g\right)k}{\rho_l+\rho_g}-\frac{g\sigma k^3}{\rho_l+\rho_g}\right]^{1/2} \tag{4}$$

According to the previous analysis, the larger the value of b_k, the more unstable the sub-disturbance, which corresponds to a greater growth rate of the boundary. Therefore, Eq. 4 indicates that the density difference and gravity play important roles in the hydraulic instability. On the contrary, surface tension tends to restrain the disturbances. When the wavelength l is small, b_k is imaginary and the corresponding disturbance will disappear.

$$\left(\frac{db_k}{dk}\right)=0\Rightarrow l=l_0=2\pi\left[\frac{3\sigma}{\left(\rho_l-\rho_g\right)g}\right]^{\frac{1}{2}} \tag{5}$$

As shown in Eq. 5, the value of b_k is a maximal real number when $l=l_0$. In this condition, the disturbance is most likely to develop into a visible bubble. This special wavelength is also called the "most dangerous wavelength".

However, the surface tension, σ, of supercritical fluids is always zero. For an arbitrary k, the value of b_k is real, which indicates that all disturbances will grow, leading to an unstable interface. Compared with the subcritical film boiling cases, the natural convection in supercritical fluid cases are more irregular and chaotic.

3 Numerical methods and models

To prove the prior theories, several numerical simulations are performed for both the subcritical and supercritical fluids. This section aims to demonstrate the numerical methods and models.

3.1 Horizontal film boiling of subcritical fluids

3.1.1 Macro-scale model

For the subcritical cases, the computational domain is a rectangular region. The domain width is the most dangerous wavelength, l_0, and the height is $3l_0$ (Figure 4). The bottom is a no-slip wall with a constant temperature. The left and right boundaries are both symmetrical. The top boundary is free, where the vapor is allowed to exit and the saturated liquid is allowed to enter.

In the initial condition, the liquid temperature is set as the saturated temperature. The gas-liquid interface is initialized as the original disturbance, which satisfies

$$y=\frac{l_0}{128}\left[4.0+\cos\left(\frac{2\pi x}{l_0}\right)\right] \tag{6}$$

Meanwhile, the vapor temperature increases linearly from the interface to the bottom, along the negative y direction.

3.1.2 Numerical methods

In order to simulate horizontal film boiling, the coupled level-set and volume-of-fluid method in FLUENT 17.2 is used to capture and track the interface. The continuum surface force model (CSF) (Brackbill et al., 1992) is used to consider the effect of surface tension in the momentum equation. As the fluid velocity is small, these cases only consider the laminar model. The governing equations for these models can be found in the help manual of Fluent.

The evaporation model is presented by Sun et al. (2012), and is developed specially for film boiling. In this model, heat transfer in the saturated liquid is ignored. Therefore, the thermal conductivity of the saturated liquid, λ_l, is set as 0, and the isobaric heat capacity of the saturated liquid is set to that of the gas. To calculate the heat flux on the interface q_S, assuming Assuming the fraction of the gas is α_g and the latent heat of vaporization is h_{lg}, then

$$q_S=2\lambda_g\left(\nabla\alpha_g\cdot\nabla T\right) \tag{7}$$

The mass transfer from the gas to liquid, $\dot{m}_l$, is calculated in Eq. 8, opposite to the mass transfer from the liquid to gas, $\dot{m}_g$.

TABLE 1 Numerical simulation cases.

Case	Fluid	Pressure/MPa	l_0/m	ΔT/K
Case 1	Water	—	0.0768	5
Case 2	Carbon dioxide	7.0	0.0025	80
Case 3	Carbon dioxide	7.37	0.0004	80

$$\dot{m}_l = -\dot{m}_g = \frac{2\lambda_g\left(\nabla\alpha_g \cdot \nabla T\right)}{h_{lg}} \tag{8}$$

Finally, through the used defined functions (UDFs) of FLUENT, $\dot{m}_l$ and $\dot{m}_g$ are respectively added to the mass conservation equations of the liquid and gas as the mass source terms. q_S is added to the energy conservation equation as an energy source term.

The numerical simulations of the cases are shown in Table 1 and the properties of the saturated liquid and vapor are listed in Table 2.

3.1.3 Grid independence tests

To obtain grid-independent results, three different grid systems of 32×96, 64×192 and 128×384 in Case 1 are considered. Figure 5A shows the bubble shapes computed on the three grids at the same time, $t = 0.6\,s$. Figure 5B presents the computed space-averaged Nusselt number changes over time on the three grids with a characteristic length $l = [\sigma/(\rho_l - \rho_g)g]^{1/2}$. According to these figures, the 64×192 grid system is suitable for this case, and is selected for the later simulations of film boiling. The time step, Δt, in all the cases is $1 \times 10^{-5}s$, as the relative difference in time- and space-averaged Nusselt numbers for $\Delta t = 5 \times 10^{-6}$ s is less than 5%.

As a verification, the results are compared with Klimenko's analyses (dashed line in Figure 5B). In Case 1, the space- and time-averaged Nusselt number is 1.70, whereas it is 1.91 according to Klimenko's correlation. The difference between them is 10% and thus the results are comparable and consistent with the prior work.

TABLE 2 Properties database for cases 1–3.

Case	-	ρ	c_P	λ	μ	σ	h_{lg}
		kg/m^3	J/(kg · K)	W/(m · K)	Pa · s	N/m	J/kg
1	Liquid	200	200.0	0	0.1	0.1	10^4
	Vapor	5	200.0	1.0	0.005		
2	Liquid	638.3	2.19×10^4	0	4.84×10^{-5}	1.72×10^{-6}	8.3×10^4
	Vapor	304.0	2.19×10^4	0.0688	2.3×10^{-5}		
3	Liquid	512.1	1.83×10^6	0	3.65×10^{-5}	1.17×10^{-6}	2.06×10^4

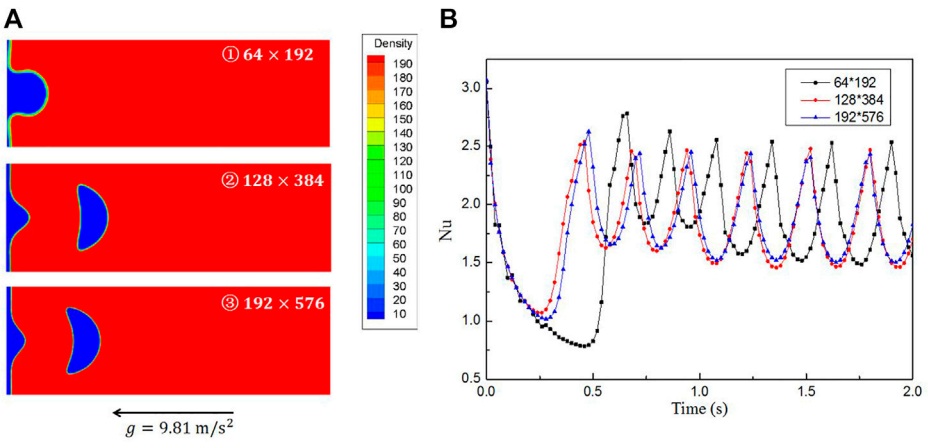

FIGURE 5
Results for three grid systems. **(A)** Bubble shapes at t = 0.6 s and **(B)** time-dependent, space-averaged Nusselt numbers.

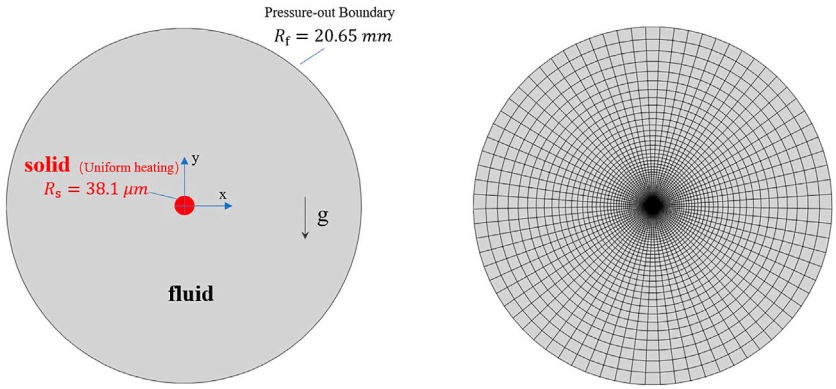

FIGURE 6
Computational domain and boundary conditions in supercritical cases.

3.2 Pseudo-boiling of supercritical fluids

3.2.1 Macro-scale model

In the pseudo-boiling cases, the bulk temperature and the heating wall temperature are below and above the pseudo-critical temperature, T_{pc}, respectively. Referring to Rousselet's experiments (Rousselet et al., 2013), the heat transfer characteristics of supercritical carbon dioxide in a simplified two-dimensional cylindrical model are studied (Figure 6).

In the model, a uniformly heated wire is present in the center, and the outer boundary is free. The computational domain is large enough so as to not affect the flow field near the wire. The radius of the wire and the domain are 38.1 μm and 20.65 mm, respectively. The pressure and temperature of the initial fluids and backflows are 7.5 MPa and 10°C, respectively.

3.2.2 Numerical methods

According to the statement in Section 2, supercritical fluids are always homogeneous with no phase transition. However, property changes with temperature in the pseudo-critical region, especially the density change, are not linear. The density can be doubled within a small temperature range, and the density change is certainly not small. Therefore, distinct from normal, natural convection simulations of single-phase fluids, the two main assumptions that the well-known Boussinesq approximation relied on are no longer valid in pseudo-boiling cases. It is thus necessary to solve the Navier-Stokes equations directly, with variable properties.

The change of the carbon dioxide properties with pressure is ignored, and only the effect of temperature is considered. The properties are described by a piecewise-linear profile consisting of 50 data points given by REFPROP. In the region where physical properties change dramatically, the temperature interval between adjacent data points is small. Similar to the subcritical boiling cases, only the laminar model is considered.

3.2.3 Independence tests

The independence tests study the effects of the number of circumferential and radial meshes and time steps. As shown in Table 3, the 76 × 120 grid system is suitable for this case, and is selected for the later simulations. Meanwhile, the wall temperature curves calculated at different time steps are almost identical (Figure 7A). The time step, Δt, of 2×10^{-4} s is suitable.

As a verification, the results are compared with Rousselt's experiments (dots in Figure 7B). For the 22 calculated conditions, the maximum relative difference of the wall temperature is approximately 18% and the mean relative difference is only 6%. Therefore, the model used in this section is reliable.

4 Results and discussions

4.1 Results of horizontal film boiling cases

Figure 8 presents six typical bubble shapes during the bubble release process for Case 2. For saturated carbon dioxide at 7 MPa, when the overheat temperature is high enough, the generated gas gathers into a stable film and film boiling occurs. With a given initial interface, the bubble formed at the center rises under the effect of buoyancy. The neck of the bubble becomes thinner until detachment. After detaching, the bubble continues to rise and leaves a packet at the detachment point (Figure 8C). This packet is pulled back into the gas film under the effect of surface tension. Further, the packet is finally absorbed and becomes a disturbance that propagates to both sides (Figure 8D). Meanwhile, the shape of the rising bubble constantly changes. As shown in Figures 8E,F, new bubble release processes occur at the original antinodes. If the flow field is undisturbed, this cycle is periodic. These results are consistent with experimental observations (Figure 9A). The photos are reproduced with permission from Abadzic and Goldstein (1970).

TABLE 3 Mesh independence tests.

Grid No.	Circumferential mesh number	Radial mesh number	T_w	Relative error (%)
1	16	120	377.7	−3.35
2	36	120	388.5	−0.59
3	76	120	390.8	0
4	116	120	391.2	0.10
5	76	80	390.3	−0.13
6	76	100	390.7	−0.03
7	76	200	390.4	−0.10

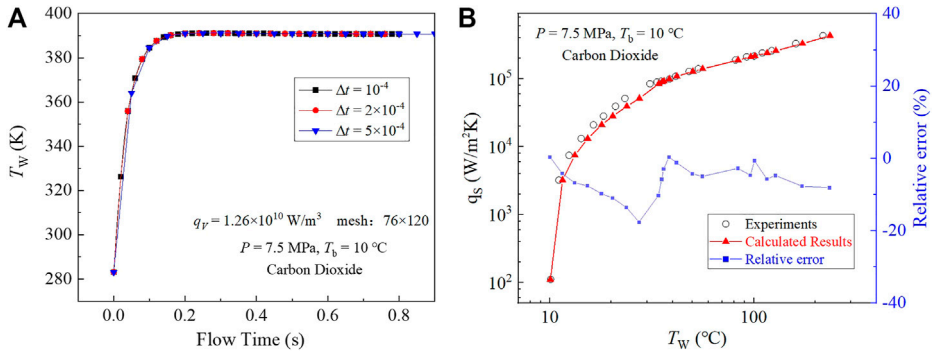

FIGURE 7
Independence tests and verifications. **(A)** Time step independence tests. **(B)** Comparisons with the experiments (Rousselet et al., 2013).

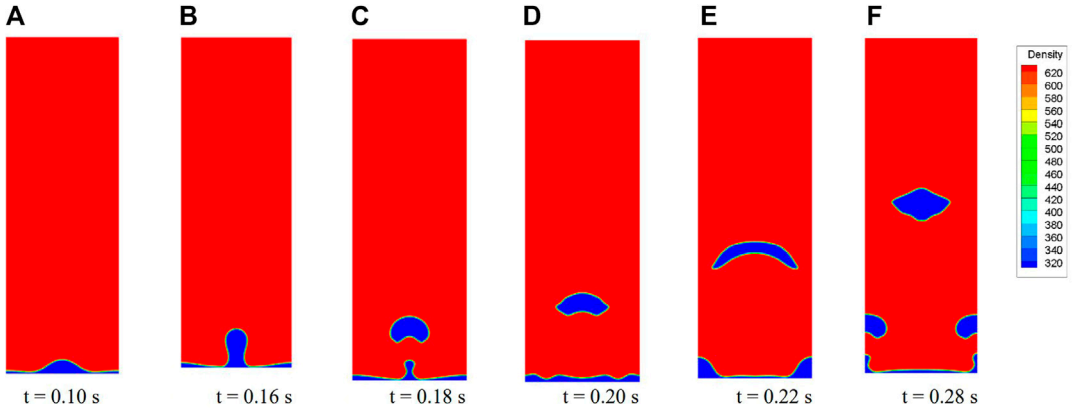

FIGURE 8
Density contours of carbon dioxide at 7.0 MPa with 80 K overheat, at different times.

In this process, the overheat condition provides the necessary energy for bubble formation and affects the frequency of bubble detachment. Specifically, when the overheat temperature is low, the whole gas film may form a bubble and the bubble then detaches from the wall. At this time, the wall is no longer covered by the vapor, and the

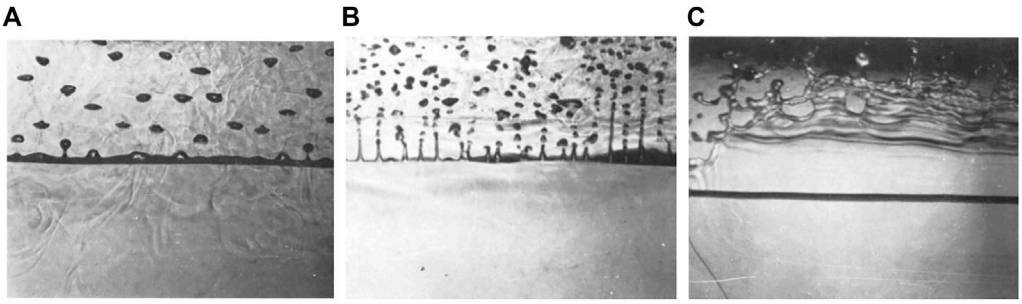

FIGURE 9
Film boiling experimental results for carbon dioxide at different cases. **(A)** 80 K overheat; **(B)** 110 K overheat; **(C)** 400 K overheat.

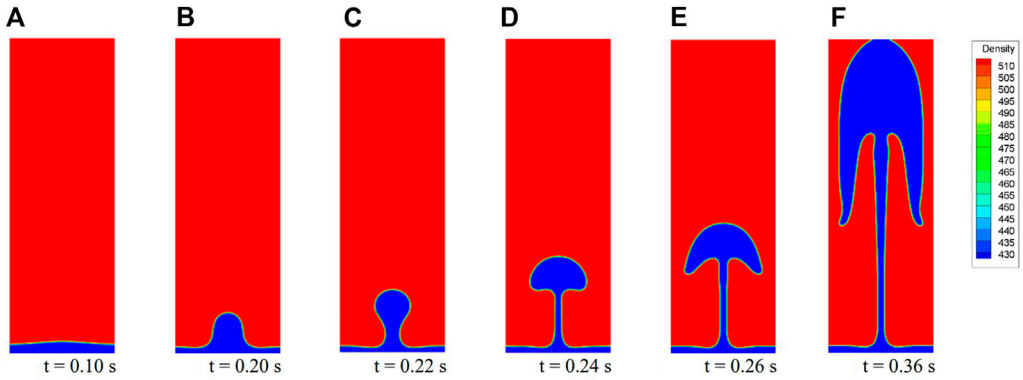

FIGURE 10
Density contours of carbon dioxide at 7.37 MPa with 80 K overheat, at different times.

boiling mode is nucleate boiling. The surface tension effect tends to generate a "smooth" interface as the surface energy decreases. According to Eq. 4, a larger value of σ leads to a smaller or even non-real value of b, corresponding to slower development of the disturbance or spontaneous decay.

When approaching the critical point, the differences between the two phases, in terms of latent heat and surface tension decrease rapidly. In Case 3, for saturated carbon dioxide at 7.37 MPa, the interface (Figure 10) is a slender column rather than individual bubbles as seen in Case 2, although the overheat temperature in the two cases are identical. At this condition, vapor formation becomes easier and numerous vapors are generated at a moderate overheat temperature. The slender vapor column becomes taller and accumulates most of the vapor at the top. Upon disturbance, the top of the vapor column may break into many small

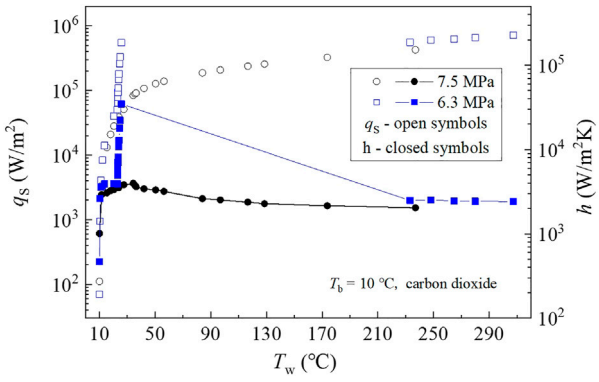

FIGURE 11
Surface heat flux and heat transfer coefficient at different wall temperatures.

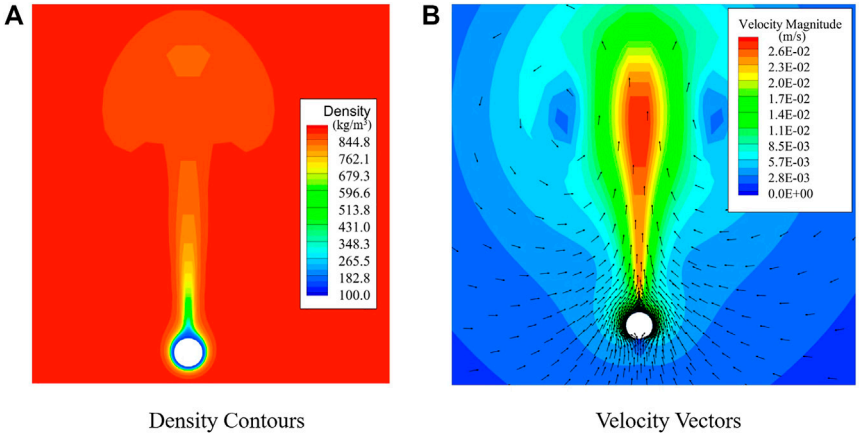

FIGURE 12
(A) Density contour and **(B)** velocity contour and vectors at 7.5 MPa with 90 K overheat.

bubbles (Figure 9B). In this context, the numerical result is too idealistic to observe.

If the vapor is produced faster, the vapor columns may converge to form a vapor sheet, which has been verified by experiment (Figure 9C).

4.2 Results of the pseudo-boiling cases

Figure 11 compares the surface heat flux, q_S, and the heat transfer coefficient, h, in supercritical and subcritical cases. The results at $P = 6.3$ MPa are from the experiments (Rousselet et al., 2013), whereas the results at $P = 7.5$ MPa are calculated based on the above proven models.

When the bulk is liquid-like, the heat transfer curve, $T_W - h$, of the supercritical carbon dioxide can be regarded as a continuation of the subcritical boiling curve. The main phenomenon is that the heat transfer mode rapidly evolves from single-phase, natural convection to "film-like boiling", while the nucleate boiling mode disappears. For similar bulk properties, the curves for the heat flux, q_S, and the heat transfer coefficient, h, in subcritical and supercritical cases, approximately overlap in some regions.

Figure 12 presents the density and velocity contours of the fully-developed pseudo-boiling case. The surface heat flux q_S is 2.14×10^5 W/m^2 and the calculated mean wall temperature is approximately 100°C, which differs from the experiment by less than 1°C.

The density profile displays a three-layer structure: the gas-like fluid layer, the transition layer, and the liquid-like fluid layer. Owing to the hydrodynamic instability, a number of initial disturbances appear in the transition layer and develop into the thermal plumes.

Thermal plumes are the key and are similar to bubbles in the subcritical cases. A typical plume exhibits a mushroom-like structure, consisting of a central rising column with vortexes on both sides. In the growth process, the upper high-density fluids are pushed away by the plume and flow downward along the sides. Some of the high-density fluid flows into the bottom low-density layer and is then heated, finally rising along the central column. The plumes may collide and merge with one another. The plumes cool as they rise, and their shapes change constantly. Specifically, the vertexes on both sides of the plumes are easily broken away, while the generated disturbances further affect the flow field.

4.3 Comparison of the pseudo-boiling and boiling cases

Thermal plumes in pseudo-boiling cases act like bubbles and vapor columns, and the near-wall low-density fluid layer is similar to the vapor film. Significant similarities exist between pseudo-boiling cases and film boiling cases, especially for the near-critical film boiling cases (Figure 10). However, in supercritical conditions, phase interfaces are non-existent, and the surface tension, σ, is reduced to zero. According to Eq. 4, at this time, b is always a real number for an arbitrary wave number m. Therefore, at an arbitrary wavelength, fluctuations will develop, and the most dangerous wavelength is non-existent. The distance between adjacent plumes can be small without restricting the subcritical conditions. Thus, the flow modes are more irregular and disordered than those in subcritical film boiling. Figure 13A (Abadzic and Goldstein, 1970) presents a visual observation of the horizontal wire heating experiment in supercritical carbon dioxide. The plume structures and the similarity to film boiling are evident.

Heat transfer in these two cases is enhanced by convection as the boundary layers are disturbed by the rising vapor or gas-like fluids. Certainly, the degree of heat transfer enhancement is

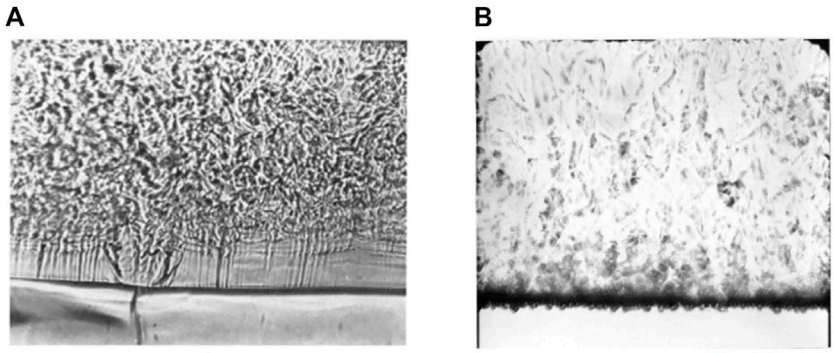

FIGURE 13
Pseudo-boiling experiments on a wire. **(A)** Pseudo film boiling **(B)** Pseudo nucleate boiling.

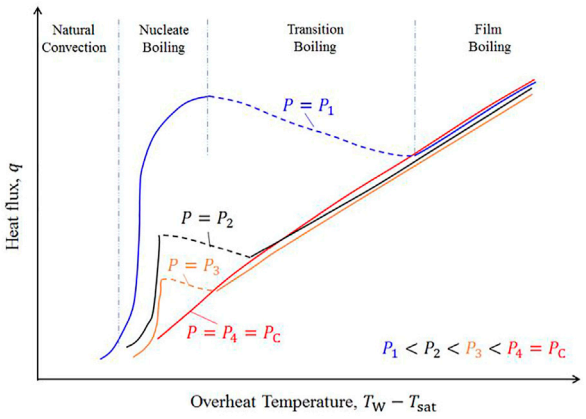

FIGURE 14
Schematic of boiling curves at different pressures.

much lower than for nucleate boiling. The low-density, near-wall fluid layer severely limits heat transfer. In applications, film boiling is regarded as the cause of heat transfer deterioration. It is desirable to avoid the transition from nucleate boiling to film boiling, which is called boiling crisis.

Many experiments have verified that heat fluxes when nucleate boiling occurs are reduced as the critical point is approached, and film boiling occurs more readily (Figure 14) (Hall and Jackson, 1978). The nucleate boiling and transition boiling areas in the boiling curve shrink, while the film boiling area expands. In this context, if only these isothermal heating cases are considered, pseudo film boiling can be regarded as an extension of near-critical boiling.

In subcritical boiling, an isothermal heating wall may lead to different boiling modes, which also depend on the heat flux, the number of vaporized cores, etc. However, according to the above analyses, pseudo film boiling is the only likelihood for an isothermal heating wall in pseudo-boiling cases. In order to prevent the formation of a low-density fluid layer, a heating wall with an inhomogeneous temperature profile is required.

Prior experiments have proved pseudo nucleate boiling, which is called bubble-like flow, and corresponds to a considerable increase in the heat transfer coefficient (Figure 13B). Pseudo nucleate boiling in the horizontal heating cases is only observed when the heaters are very fine wires with low thermal diffusion coefficients, for example, a nichrome wire with diameter of 0.1 mm (Knapp and Sabersky, 1966). Theoretically, a material with a low thermal diffusion coefficient is more likely to have an inhomogeneous surface temperature. Bubble-like structures are generated and released from hotspots. The hotspots are then covered and cooled by the high-density and low-temperature bulk. Nevertheless, the explanation provided in this paper is not insufficient. More experiments with wires of different diameters and materials are required to provide further evidence for our theory.

5 Conclusion

This paper theoretically analyses the similarities and differences between the subcritical gas-liquid transition and the pseudocritical transition. The heat transfer characteristics in the subcritical gas-liquid transition and the pseudocritical transition are compared through theory and numerical simulations.

Property changes during the subcritical phase transition and the pseudocritical transition are similar, leading to similar heat transfer characteristics. The similarities are the result of the hydraulic instability of the low-density bulk under the effects of gravity. However, thermodynamic stability prevents the phase separation of supercritical fluids. Pseudocritical transition only depends on the temperature; the formation of low-density bulk in supercritical cases is a deterministic process. On the contrary,

vapor formation in subcritical cases is a stochastic process which relies on the initial nucleation sites.

The random distribution of nucleation sites means that the heating wall may not necessarily be completely covered by the low-density fluid during boiling. For an isothermal heating wall, different boiling modes may appear in subcritical cases, whereas only pseudo film boiling is observed in supercritical cases. For isothermal heating cases, pseudo-boiling cases can be regarded as an extension of near-critical boiling. However, pseudo nucleate boiling may appear in non-isothermal cases, which strongly depends on the heater geometry, materials, etc.

Data availability statement

The original contributions presented in the study are included in the article/Supplementary Material, further inquiries can be directed to the corresponding author.

Author contributions

ML: software, methodology, writing-original draft; SL: methodology; DX: analysis; SH: methodology, supervision, YH: conceptualization, funding acquisition, supervision.

Funding

This work was supported by the National Natural Science Foundation of China (Grant No. U1867218) and the Nuclear Power Technology Innovation Center in the National Defense Science and Technology Industry of China.

Conflict of interest

The authors declare that the research was conducted in the absence of any commercial or financial relationships that could be construed as a potential conflict of interest.

Publisher's note

All claims expressed in this article are solely those of the authors and do not necessarily represent those of their affiliated organizations, or those of the publisher, the editors and the reviewers. Any product that may be evaluated in this article, or claim that may be made by its manufacturer, is not guaranteed or endorsed by the publisher.

References

Abadzic, E., and Goldstein, R. J. (1970). Film boiling and free convection heat transfer to carbon dioxide near the critical state. *Int. J. Heat Mass Transf.* 13 (7), 1163–1175. doi:10.1016/0017-9310(70)90006-2

Ackerman, J. (1970). Pseudoboiling heat transfer to supercritical pressure water in smooth and ribbed tubes. *J. Heat. Transf.* 92 (3), 490–497. doi:10.1115/1.3449698

Ahn, Y., Bae, S. J., Kim, M., Cho, S. K., Baik, S., Lee, J. I., et al. (2015). Review of supercritical CO2 power cycle technology and current status of research and development. *Nucl. Eng. Technol.* 47 (6), 647–661. doi:10.1016/j.net.2015.06.009

Banuti, D. T., and Hannemann, K. (2014). "Supercritical pseudo-boiling and its relevance for transcritical injection," in 50th AIAA/ASME/SAE/ASEE Joint Propulsion Conference, Cleveland, OH, July 28-30, 2014.

Berenson, P. J. (1961). Film-boiling heat transfer from a horizontal surface. *J. Heat Transf.* 83 (3), 351–356. doi:10.1115/1.3682280

Boukari, H., Shaumeyer, J. N., Briggs, M. E., and Gammon, R. W. (1990). Critical speeding up in pure fluids. *Phys. Rev. A . Coll. Park.* 41 (4), 2260–2263. doi:10.1103/physreva.41.2260

Brackbill, J. U., Kothe, D. B., and Zemach, C. (1992). A continuum method for modeling surface tension. *J. Comput. Phys.* 100 (2), 335–354. doi:10.1016/0021-9991(92)90240-y

Brun, K., Friedman, P., and Dennis, R. (2017). *Fundamentals and applications of supercritical carbon dioxide (sCO2) based power cycles*. Sawston, United Kingdom: Woodhead publishing.

Cardy, J. (1996). *Scaling and renormalization in statistical physics*. NewYork: Cambridge University Press.

Duffey, R. B., and Pioro, I. L. (2005). Experimental heat transfer of supercritical carbon dioxide flowing inside channels (survey). *Nucl. Eng. Des.* 235 (8), 913–924. doi:10.1016/j.nucengdes.2004.11.011

Fomin, Y. D., Ryzhov, V., Tsiok, E., and Brazhkin, V. (2015). Dynamical crossover line in supercritical water. *Sci. Rep.* 5, 14234. doi:10.1038/srep14234

Fu, Y., Huang, H., Wen, J., Xu, G., and Zhao, W. (2017). Experimental investigation on convective heat transfer of supercritical RP-3 in vertical miniature tubes with various diameters. *Int. J. Heat Mass Transf.* 112, 814–824. doi:10.1016/j.ijheatmasstransfer.2017.05.008

Goldstein, R. J., and Aung, W. (1968). Heat transfer by free convection from a horizontal wire to carbon dioxide in the critical region. *J. Heat Transf.* 90 (1), 51–55. doi:10.1115/1.3597459

Gorelli, F., Santoro, M., Scopigno, T., Krisch, M., and Ruocco, G. (2006). Liquidlike behavior of supercritical fluids. *Phys. Rev. Lett.* 97 (24), 245702. doi:10.1103/PhysRevLett.97.245702

Gu, H., Li, H., Wang, H., and Luo, Y. (2013). Experimental investigation on convective heat transfer from a horizontal miniature tube to methane at supercritical pressures. *Appl. Therm. Eng.* 58 (1-2), 490–498. doi:10.1016/j.applthermaleng.2013.04.049

Ha, M. Y., Yoon, T. J., Tlusty, T., Jho, Y., and Lee, W. B. (2018). Widom delta of supercritical gas–liquid coexistence. *J. Phys. Chem. Lett.* 9 (7), 1734–1738. doi:10.1021/acs.jpclett.8b00430

Hahne, E., and Neumann, R. (1981). Boiling-like phenomena in free-convection heat transfer at supercritical pressures. *Warme- Stoffubertragung* 15 (3), 171–180. doi:10.1007/BF01376829

Hall, W. B., and Jackson, J. D. (1978). Heat transfer near the critical point. *Adv. Heat. Transf.* 7, 1–86. doi:10.1016/S0065-2717(08)70016-9

Hiroaki, T., Ayao, T., Masaru, H., and Nuchi, N. (1973). Effects of buoyancy and of acceleration owing to thermal expansion on forced turbulent convection in vertical circular tubes—Criteria of the effects, velocity and temperature profiles, and reverse transition from turbulent to laminar flow. *Int. J. Heat Mass Transf.* 16 (6), 1267–1288. doi:10.1016/0017-9310(73)90135-x

Jiang, P., Liu, B., Zhao, C., and Luo, F. (2013). Convection heat transfer of supercritical pressure carbon dioxide in a vertical micro tube from transition to turbulent flow regime. *Int. J. heat mass Transf.* 56 (1-2), 741–749. doi:10.1016/j.ijheatmasstransfer.2012.08.038

Kadanoff, L. P., Götzes, W., Hamblen, D., Hecht, R., Kane, J., Palciauskas, V. V., et al. (1967). Static phenomena near critical points: Theory and experiment. *Rev. Mod. Phys.* 39 (2), 395–431. doi:10.1103/RevModPhys.39.395

Knapp, K. K., and Sabersky, R. H. (1966). Free convection heat transfer to carbon dioxide near the critical point. *Int. J. Heat Mass Transf.* 9 (1), 41–51. doi:10.1016/0017-9310(66)90055-x

Li, Z., Jiang, P., Zhao, C., and Zhang, Y. (2010). Experimental investigation of convection heat transfer of CO2 at supercritical pressures in a vertical circular tube. *Exp. Therm. fluid Sci.* 34 (8), 1162–1171. doi:10.1016/j.expthermflusci.2010.04.005

Liu, M., Tang, J., Liu, S., Xi, D., Min, L., Zang, J., et al. (2022). Modified landau model for fluids: A rethink of pseudoboiling theory for supercritical fluids. *J. Supercrit. Fluids* 183, 105554. doi:10.1016/j.supflu.2022.105554

Liu, S., Huang, Y., Liu, G., Wang, J., and Leung, L. K. (2017). Improvement of buoyancy and acceleration parameters for forced and mixed convective heat transfer to supercritical fluids flowing in vertical tubes. *Int. J. Heat Mass Transf.* 106, 1144–1156. doi:10.1016/j.ijheatmasstransfer.2016.10.093

Maxim, F., Karalis, K., Boillat, P., Banuti, D. T., Marquez Damian, J. I., Niceno, B., et al. (2020). Thermodynamics and dynamics of supercritical water pseudo-boiling. *Adv. Sci. (Weinh).* 8, 2002312. doi:10.1002/advs.202002312

McEligot, D., Coon, C., and Perkins, H. (1970). Relaminarization in tubes. *Int. J. Heat Mass Transf.* 13 (2), 431–433. doi:10.1016/0017-9310(70)90118-3

Mokry, S., Pioro, I., Kirillov, P., and Gospodinov, Y. (2010). Supercritical-water heat transfer in a vertical bare tube. *Nucl. Eng. Des.* 240 (3), 568–576. doi:10.1016/j.nucengdes.2009.09.003

Nasuti, F., and Pizzarelli, M. (2020). Pseudo-boiling and heat transfer deterioration while heating supercritical liquid rocket engine propellants. *J. Supercrit. Fluids* 168, 105066. doi:10.1016/j.supflu.2020.105066

Neumann, R. J., and Hahne, E. W. (1980). Free convective heat transfer to supercritical carbon dioxide. *Int. J. Heat Mass Transf.* 23 (12), 1643–1652. doi:10.1016/0017-9310(80)90223-9

Nishkawa, K., and Ito, T. (1969). An analysis of free-convective heat transfer from an isothermal vertical plate to supercritical fluids. *Int. J. Heat Mass Transf.* 12 (11), 1449–1463. doi:10.1016/0017-9310(69)90027-1

Onuki, A., Hao, H., and Ferrell, R. A. (1990). Fast adiabatic equilibration in a single-component fluid near the liquid-vapor critical point. *Phys. Rev. A . Coll. Park.* 41 (4), 2256–2259. doi:10.1103/physreva.41.2256

Petukhov, B., Protopopov, V., and Silin, V. (1972). Experimental investigation of worsened heat-transfer conditions with the turbulent flow of carbon dioxide at supercritical pressure. *High. Temp.* 10 (2), 304–310.

Pioro, I. L., and Duffey, R. B. (2005). Experimental heat transfer in supercritical water flowing inside channels (survey). *Nucl. Eng. Des.* 235 (22), 2407–2430. doi:10.1016/j.nucengdes.2005.05.034

Rousselet, Y., Warrier, G. R., and Dhir, V. K. (2013). Natural convection from horizontal cylinders at near-critical pressures—part I: Experimental study. *J. Heat Transf.* 135 (2). doi:10.1115/1.4007672

Shen, B., and Zhang, P. (2013). An overview of heat transfer near the liquid–gas critical point under the influence of the piston effect: Phenomena and theory. *Int. J. Therm. Sci.* 71, 1–19. doi:10.1016/j.ijthermalsci.2013.04.010

Simeoni, G., Bryk, T., Gorelli, F., Krisch, M., Ruocco, G., Santoro, M., et al. (2010). The Widom line as the crossover between liquid-like and gas-like behaviour in supercritical fluids. *Nat. Phys.* 6 (7), 503–507. doi:10.1038/nphys1683

Sun, D., Xu, J., and Wang, L. (2012). A vapor-liquid phase change model for two-phase boiling and condensation. *J. Xi'an Jiaot. Univ.* 46 (7), 7–11.

Swenson, H., Carver, J., and Kakarala, C. d. (1965). Heat transfer to supercritical water in smooth-bore tubes. *J. Heat Transf.* 87 (4), 477–483. doi:10.1115/1.3689139

Taylor, G. I. (1950). "The instability of liquid surfaces when accelerated in a direction perpendicular to their planes. I," in Proceedings of the Royal Society of London. Series A. Mathematical and Physical Sciences, Taylor, Geoffrey, March 1950.

Wilson, K. G. (1971). Renormalization group and critical phenomena. I. Renormalization group and the kadanoff scaling picture. *Phys. Rev. B* 4 (9), 3174–3183. doi:10.1103/PhysRevB.4.3174

Xu, J., Zhang, H., Zhu, B., and Xie, J. (2020). Critical supercritical-boiling-number to determine the onset of heat transfer deterioration for supercritical fluids. *Sol. Energy* 195, 27–36. doi:10.1016/j.solener.2019.11.036

Xu, R.-N., Luo, F., and Jiang, P.-X. (2017). Buoyancy effects on turbulent heat transfer of supercritical CO2 in a vertical mini-tube based on continuous wall temperature measurements. *Int. J. heat mass Transf.* 110, 576–586. doi:10.1016/j.ijheatmasstransfer.2017.03.063

Yoon, T. J., Ha, M. Y., Lee, W. B., and Lee, Y.-W. (2019). A corresponding-state framework for the structural transition of supercritical fluids across the Widom delta. *J. Chem. Phys.* 150 (15), 154503. doi:10.1063/1.5086467

Zappoli, B., Bailly, D., Garrabos, Y., Neindre, B. L., Guenoun, P., and Beysens, D. (1990). Anomalous heat transport by the piston effect in supercritical fluids under zero gravity. *Phys. Rev. A . Coll. Park.* 41 (4), 2264–2267. doi:10.1103/physreva.41.2264

Nomenclature

P pressure, MPa
T temperature, K
V volume, m^3
m mass, kg
t time, s
ρ density, kg/m^3
c_P isobaric heat capacity, $kJ/(kg \cdot K)$
λ thermal conductivity, $W/(m \cdot K)$
μ viscosity, Pa·s
κ_T isothermal compressibility, 1/MPa
α_P thermal expansion rate, 1/K
σ surface tension, N/m
h_{lg} latent heat of vaporization, J/kg
η distance perpendicular to liquid-vapor interface, m
k wave number, 1/m
l wavelength, m
n wave frequency, 1/s
b -in growth coefficient, 1/s
l_0 most dangerous wavelength, m
q heat flux, W/m^2
q_S heat flux on the interface, W/m^2
α volume fraction of vapor
Nu Nusselt number
h heat transfer coefficient

Subscripts

pc pseudocritical
C critical
l liquid
g vapor or gas
b bulk
w wall
sat saturation